

This is the **accepted version** of the journal article:

Shen, Xiangjin; Shen, Miaogen; Wu, Chaoyang; [et al.]. «Critical role of water conditions in the responses of autumn phenology of marsh wetlands to climate change on the Tibetan Plateau». *Global change biology*, Vol. 30, issue 1 (Jan. 2023), art. e17097. DOI 10.1111/gcb.17097

This version is available at <https://ddd.uab.cat/record/287436>

under the terms of the  **CC BY** license

1 **Critical role of water conditions in the responses of autumn**
2 **phenology of marsh wetlands to climate change on the Tibetan**
3 **Plateau**

4 Xiangjin Shen¹, Miaogen Shen², Chaoyang Wu³, Josep Peñuelas^{4,5}, Philippe Ciais⁶, Jiaqi
5 Zhang¹, Chris Freeman⁷, Paul I. Palmer^{8,9}, Binhui Liu¹⁰, Mark Henderson¹¹, Zhaoliang
6 Song¹², Shaobo Sun¹², Xianguo Lu¹, Ming Jiang¹

7 ¹Northeast Institute of Geography and Agroecology, Chinese Academy of Sciences,
8 Changchun, China.

9 ²State Key Laboratory of Earth Surface Processes and Resource Ecology, Faculty of
10 Geographical Science, Beijing Normal University, Beijing, China.

11 ³Institute of Geographic Sciences and Natural Resources Research, Chinese Academy of
12 Sciences, Beijing, China.

13 ⁴CREAF, Cerdanyola del Vallès, Barcelona, Spain.

14 ⁵CSIC, Global Ecology Unit CREAM-CSIC- UAB, Barcelona, Spain.

15 ⁶Laboratoire des Sciences du Climat et de l'Environnement, LSCE/IPSL, CEA-CNRS-
16 UVSQ, Université Paris-Saclay, Gif-sur-Yvette, France.

17 ⁷School of Natural Sciences, Bangor University, Bangor LL57 2UW, UK.

18 ⁸School of GeoSciences, University of Edinburgh, Edinburgh, UK.

19 ⁹National Centre for Earth Observation, University of Edinburgh, Edinburgh, UK.

20 ¹⁰College of Forestry, Northeast Forestry University, Harbin, China.

21 ¹¹Public Policy Program and Environmental Studies Program, Mills College, Oakland,
22 California, USA.

23 ¹²Institute of Surface-Earth System Science, School of Earth System Science, Tianjin
24 University, Tianjin, China.

25

26

27 Abstract:

28 The Tibetan Plateau, housing 20% of China's wetlands, plays a vital role in the regional
29 carbon cycle. Examining the phenological dynamics of wetland vegetation in response to
30 climate change is crucial for understanding its impact on the ecosystem. Despite this
31 importance, the specific effects of climate change on wetland vegetation phenology in
32 this region remain uncertain. In this study, we investigated the influence of climate change
33 on the end of the growing season (EOS) of marsh wetland vegetation across the Tibetan
34 Plateau. Utilizing satellite-derived Normalized Difference Vegetation Index (NDVI) data
35 and observational climate data, we observed a significant delay in the regionally averaged
36 EOS of marsh vegetation by 4.10 days/decade from 2001 to 2020. Warming pre-season
37 temperatures were found to be the primary driver behind the delay in the EOS of marsh
38 vegetation, whereas pre-season cumulative precipitation showed no significant impact.
39 Interestingly, the responses of EOS to climate change varied spatially across the plateau,
40 indicating a regulatory role for hydrological conditions in marsh phenology. In the humid
41 and cold central regions, pre-season daytime warming significantly delayed the EOS.
42 However, areas with lower soil moisture exhibited a weaker or reversed delay effect,
43 suggesting complex interplays between temperature, soil moisture, and EOS. Notably, in
44 the arid southwestern regions of the plateau, increased pre-season rainfall directly delayed
45 the EOS, while higher daytime temperatures advanced it. Our results emphasize the

46 critical role of hydrological conditions, specifically soil moisture, in shaping marsh EOS
47 responses in different regions. Our findings underscore the need to incorporate
48 hydrological factors into terrestrial ecosystem models, particularly in cold and dry regions,
49 for accurate predictions of marsh vegetation phenological responses to climate change.
50 This understanding is vital for informed conservation and management strategies in the
51 face of current and future climate challenges.

52

53 **KEYWORDS** Marsh vegetation, autumn phenology, climate change, water condition,
54 Tibetan Plateau

55

56 **1 Introduction**

57 Vegetation phenology refers to the seasonal timing of life cycle events in plants and
58 reflects the dynamic responses of terrestrial ecosystems to global climate change (Chen
59 et al., 2017; Peñuelas et al., 2001; Piao et al., 2007, 2008, 2019; Richardson et al., 2013;
60 Wu et al., 2022). Several studies have demonstrated that autumn phenology, signaling the
61 end of the growing season (EOS), reflects the vegetation's growing period better than
62 spring phenology and has a significant effect on carbon sequestration in terrestrial
63 ecosystems (Bao et al., 2020; Fu et al., 2018; Garonna et al., 2014; Zhu et al., 2012).

64 Global climate change has significantly changed the autumn phenology worldwide,
65 affecting the regional and global energy balance, water flux, and carbon budget (Che et
66 al., 2014; Estiarte et al., 2015; Kelsey et al., 2021; Richardson et al., 2013; Yang et al.,

2021). Although the variations in the autumn phenology of vegetation and its response to regional and global climate changes have been extensively analyzed, most studies have focused on grassland or forest ecosystems, with few investigations of wetland ecosystems (Coleman et al., 2022; Ge et al., 2015; Ma et al., 2022; Rice et al., 2018; Yang et al., 2015). Due to the unique environmental conditions in wetlands, climate change may have different effects on the autumn phenology of vegetation compared to other ecosystems (Keppeler et al., 2021; Ma et al., 2022; Molino et al., 2022; Shen et al., 2022). Such differences must be considered if we are to better understand the responses of the global carbon cycle and ecosystem vegetation to climatic variation in the context of global climate change.

As the highest plateau in the world, the Tibetan Plateau is highly sensitive to climate change. And yet the roles of temperature or precipitation in determining the vegetation phenology of the Tibetan Plateau appear contradictory; Some studies assert that temperature plays a dominant role in determining vegetation phenology (Yu et al., 2010), while others argue that precipitation is critical to the vegetation phenology of the region (Shen et al., 2014, 2015a). Known as the “water tower of Asia”, the Tibetan Plateau features a large area of marsh wetlands with relatively high water content (Che et al., 2014; Shen et al., 2011; Shen et al., 2021a) that provide an ideal opportunity for clarifying the dominant effects of temperature and precipitation on the phenology of the vegetation of the Tibetan Plateau.

Recent studies have analyzed the effects of climate change on autumn phenology in

88 various ecosystems of the region (Shen et al., 2022b), reported the phenology of grassland
89 vegetation as positively correlated with precipitation and negatively correlated with
90 daytime maximum temperature. Increased precipitation can enhance the water use
91 efficiency of grassland vegetation, potentially delaying the EOS (Shen et al., 2015b; Wu
92 et al., 2018). However, an increase in daytime maximum temperature also promotes
93 evaporation, reducing water use efficiency and consequently advancing the EOS. Clearly,
94 an improved understanding of the influence of climate variation on the autumn phenology
95 of marsh vegetation in this region can greatly improve our knowledge of the relationships
96 between the vegetation of ecosystems and climate change.

97 This study utilizes data from 2001 to 2020, incorporating the Normalized Difference
98 Vegetation Index (NDVI) and observational climate data. The aim is to explore
99 spatiotemporal variations in the end of the growing season (EOS) and vegetation
100 responses to climatic variations in the marshes of the Tibetan Plateau. The objective is to
101 enhance our understanding and predictive capabilities regarding phenological changes in
102 marsh vegetation. By illuminating the intricate relationship between vegetation and
103 climate change in this ecologically significant area, our study's findings can offer valuable
104 new insights for ecological management and conservation efforts.

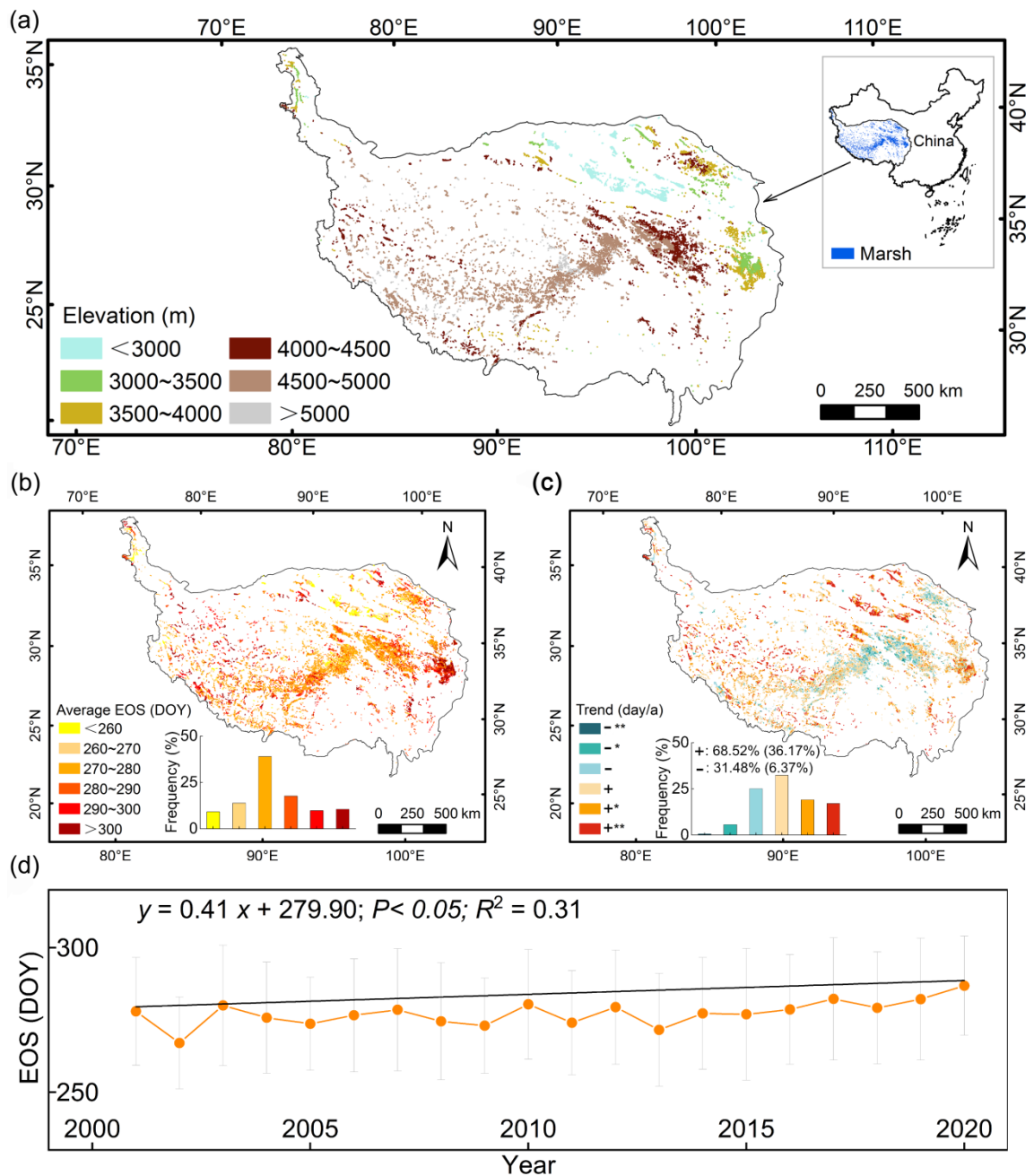
105

106 **2 Material and method**

107 2.1 Study region

108 The Tibetan Plateau is located in southwestern China at an altitude of 3,000–5,000 m

109 (average altitude > 4,000 m) and is characterized by a semi-arid and cold climate (Figure
 110 1) (Shen et al., 2022). The annual precipitation exceeds 1,000mm in the southeastern
 111 region and is < 100mm in the northwestern region (Cheng et al., 2021; Gao et al., 2013;
 112 Piao et al., 2006a). The average temperature in the northwestern and southeastern areas
 113 is approximately -6°C and 20°C , respectively (Qin et al., 2022).



114

115 FIGURE 1 Spatiotemporal change of the end of the growing season (EOS) in the marshes
116 of the Tibetan Plateau from 2001 to 2020. (a) Distribution of marshes at different altitudes
117 on the Tibetan Plateau. (b) Spatial patterns of regionally averaged EOS. (c) Temporal
118 trends in EOS. (d) Temporal variations of regionally averaged EOS. The inset histograms
119 at the bottom of (b) and (c) describe the frequency distributions of the average EOS and
120 EOS trend. - and + in C show the negative (advancing) and positive (delaying) trend,
121 respectively; * and ** indicate the trend is significant ($P < 0.05$) and extremely significant
122 ($P < 0.01$), respectively. The error bar and bold black line in D show standard error and
123 linear trend of the regionally averaged EOS, respectively.

124 As the highest plateau in the world, the Tibetan Plateau is extremely sensitive to
125 climate change (Dong et al., 2012; Zhang et al., 2013). Changes in vegetation phenology
126 in this region serve as crucial indicators of global climate change (Chen et al., 2015).
127 Large wetland areas characterized by marshes are distributed on the Tibetan Plateau and
128 are important for the ecological security of the region and the major river systems that
129 originate there, including the Huanghe (Yellow), Changjiang (Yangzi), and Brahmaputra
130 rivers. The main species of marsh plants distributed on the Tibetan Plateau are *Phragmites*
131 *australis*, *Blysmus sinocompressus*, *Carex pseudosupina*, and *Kobresia littledalei* (Shen
132 et al., 2021a).

133

134 2.2 Data

135 Satellite-derived NDVI data covering the 2001–2020 period were obtained from the

136 MOD13Q1 NDVI dataset, with temporal and spatial resolutions of 16 d and 250 m,
137 respectively (Shen et al., 2023). This dataset was provided by the Earth Science Data
138 Systems of the National Aeronautics and Space Administration.

139 The distribution of marshes in the study area was obtained from the wetland
140 distribution datasets for China for years 2000 and 2015 at a resolution of 30 m × 30 m
141 (Mao et al., 2020). These digital maps were available from the National Earth System
142 Science Data Center. The accuracy of datasets had been verified through field
143 observations, and the producer's and user's accuracies were over 95% and 98%,
144 respectively (Mao et al., 2020). We used the marsh distribution data for two specific years
145 (2000 and 2015) to extract the unchanged marsh distribution (Shen et al., 2023).

146 The soil moisture data used in this study were extracted from a 1-km daily soil
147 moisture dataset of in situ measurements conducted in China from 2000 to 2020 (Li et al.,
148 2022). These dataset was produced using spatially dense in situ observations and machine
149 learning, and was obtained from the National Tibetan Plateau Scientific Data Center.

150 The Climate Change Research Center of the Chinese Academy of Sciences provided
151 the daily gridded climate data from more than 2400 meteorological stations distributed
152 across China. These included daily precipitation as well as the minimum, maximum, and
153 mean temperatures with a spatial resolution of 1 km from 2001 to 2020. Marsh
154 distribution, soil moisture, and climatic data were resampled at a resolution of 250 m ×
155 250 m to maintain consistency with the spatial resolution of the NDVI data (Shen et al.,
156 2021b).

157

158 2.3 Methods

159 Considering that snow cover decreases the NDVI value, consequently affecting the
160 accuracy of satellite-derived phenology data, we replaced the snow-contaminated NDVI
161 values with the median value of the uncontaminated winter NDVI values between
162 November and the following March for each pixel (Shen et al., 2014, 2015). This
163 preprocessing of data has been validated and included in numerous previous studies
164 (Ganguly et al., 2010; Shen et al., 2015a; Wang et al., 2021). Based on previous research
165 (Cong et al., 2013; Liu et al., 2016; Ma et al., 2021; Piao et al., 2006b; Shen et al., 2016;
166 Su et al., 2022), we used the poly fit-maximum approach to extract phenological
167 information (Piao et al., 2006b). In this method, the growth curve of the growing season
168 is fitted with a daily temporal resolution in order to remove abnormal NDVI values (Piao
169 et al., 2006b, 2011), and the EOS date is set to correspond to the time of the largest
170 decrease in NDVI at the end of the growth period. The polyfit-maximum method has been
171 widely used to extract vegetation phenology owing to its excellent performance (Fu et al.,
172 2014; Ma et al., 2022; Piao et al., 2006b, 2011; Shen et al., 2018, 2019, 2023; Su et al.,
173 2022) and consists in a number of steps.

174 First, we calculated the annual and multiyear average rates of NDVI variation to
175 obtain the corresponding day of the year (DOY) for the vegetation's EOS (Piao et al.,
176 2006b). The following equation was used to calculate the rate of NDVI variation:

177
$$\text{NDVI}_{\text{ratio}}(t) = \frac{\text{NDVI}(t+1) - \text{NDVI}(t)}{\text{NDVI}(t)} \quad (1)$$

178 where t is time (temporal resolution of 16 days), $NDVI_{ratio}(t)$ is the rate of NDVI
 179 change corresponding to period t , $NDVI(t)$ is the NDVI value for period t , and $NDVI(t+1)$
 180 is the NDVI value for period $t+1$. We detected the time t with the minimum $NDVI_{ratio}$
 181 and used the corresponding $NDVI(t+1)$ at time $(t+1)$ as the NDVI threshold for the EOS.

182 Then, we used the maximum value method of multivariate fitting to construct a
 183 unary sixth-degree polynomial function (Piao et al., 2006b) and fitted the annual and
 184 multiyear average daily NDVI fitting curve by pixel. The formula used was:

$$185 \quad NDVI = a + a_1x^1 + a_2x^2 + a_3x^3 + a_4x^4 + a_5x^5 + a_6x^6 \quad (2)$$

186 where x is the day of each year (DOY); and $a_1, a_2, a_3, \dots, a_6$ are the regression
 187 coefficients determined by least-squares regression.

188 Finally, we substituted the DOY into the fitting curve of the multiyear average daily
 189 NDVI to obtain the NDVI threshold corresponding to the EOS (Piao et al., 2006b). We
 190 applied the NDVI threshold values to the daily NDVI fitting curve of each year to obtain
 191 the corresponding EOS values for marsh vegetation in that year.

192 To analyze the EOS trend and climatic variables on the Tibetan Plateau from 2001
 193 to 2020, we performed a linear regression analysis using the following equation (Piao et
 194 al., 2011):

$$195 \quad \theta_{slope} = \frac{(n \times \sum_{i=1}^n i \times x_i) - (\sum_{i=1}^n i \sum_{i=1}^n x_i)}{n \times \sum_{i=1}^n i^2 - (\sum_{i=1}^n i)^2} \quad (3)$$

196 where n is the number of years analyzed (i.e., 20 years for this study); θ_{slope} indicates
 197 the trend (of the EOS or climatic variables) for each pixel; and x_i is the climate variable
 198 (or EOS) during the i year. A negative θ_{slope} implies that the temporal variation shows an

199 advancing (i.e., decreasing) trend, whereas a positive θ_{slope} implies a delaying (i.e.,
200 increasing) trend.

201 To investigate the seasonal changes in the EOS in response to climate variations, we
202 analyzed the simple correlation coefficients between monthly and seasonal climate
203 factors and the EOS in previous winter (November to February of the following year),
204 spring (March to May), summer (June to August), and autumn (September to October).
205 In addition, we carried out a partial correlation analysis to further examine correlations
206 between climate variables and the EOS. Through this analysis, it was possible to
207 determine the relationship between two parameters after removing the influence of other
208 factors (Peng et al., 2013; Shen et al., 2016).

209 The partial correlation coefficient between the time series of the EOS and daytime
210 maximum temperature (or nighttime minimum temperature) was calculated to assess the
211 effect of maximum temperature (or minimum temperature) on the EOS, with precipitation
212 and minimum temperature (or maximum temperature) as the controlling variables. In line
213 with previous studies, the duration of the preseason was calculated for the maximum
214 temperature (or minimum temperature) based on the period preceding the long-term
215 average date of the EOS. When the maximum temperature (or minimum temperature) had
216 the highest absolute value for the partial correlation coefficient with the EOS, this period
217 is referred to as the preseason for the maximum temperature (Shen et al., 2016; Wu et al.,
218 2018) (or the minimum temperature). In this study, an interval of 10 days was adopted to
219 determine the duration of the preseason period and smooth out potential extreme values

220 (Shen et al., 2015a).

221 The effect of preseason cumulative precipitation on the EOS was similarly analyzed,
222 and preseason precipitation was determined by setting the maximum and minimum
223 temperatures as the controlling variables (Shen et al., 2016). We did not constrain the
224 duration of preseason precipitation to be equal to that of preseason temperature. In
225 addition, to further analyze the influences of climatic variations on the EOS, we compared
226 the partial correlation coefficients between the EOS and preseason precipitation and
227 between the EOS and maximum and minimum temperatures at different levels of soil
228 moisture.

229

230 **3 Results**

231 3.1 Spatial and temporal variations in the EOS

232 The multiyear mean EOS on the Tibetan Plateau occurred primarily between 260th and
233 300th day of year (DOY), with a regional average of 277th DOY (October 4, or October
234 3 in leap years) (Figure 1b). The EOS was later in the low altitude (below 4,000 m) humid
235 areas of the eastern Tibetan Plateau and earlier in the high-altitude (above 4,000 m)
236 central areas (Figure 1a,b).

237 The regionally averaged EOS from 2001 to 2020 across the Tibetan Plateau
238 exhibited a significant delay of 4.10 days per decade ($P < 0.05$) (Figure 1d). The
239 percentage of pixels showing a trend of delayed EOS (68.5%, with a significant
240 proportion of 36.2%, $P < 0.05$) was higher than that showing a trend of advanced EOS

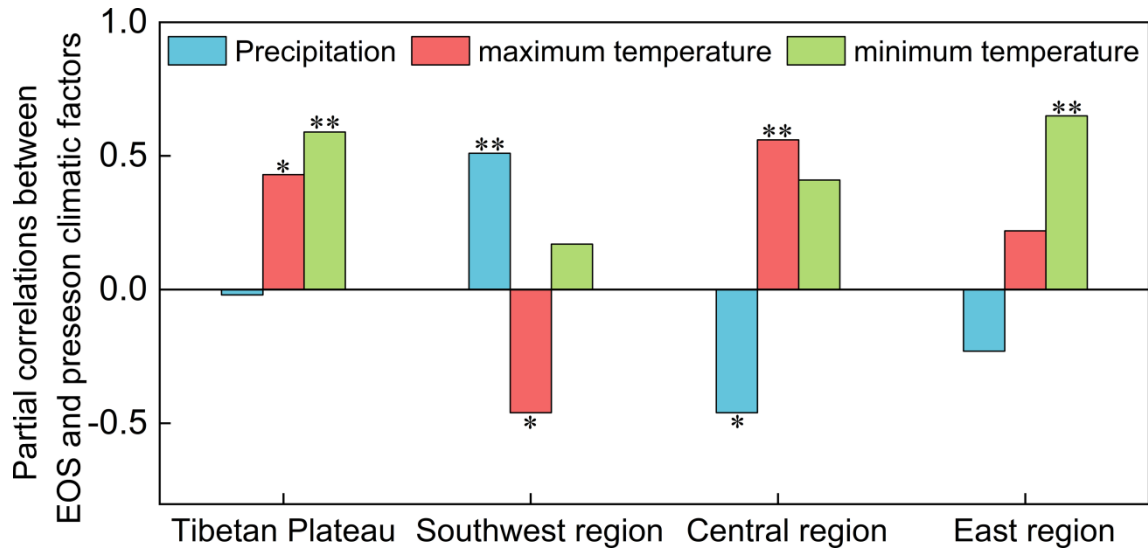
241 (31.5%, with a significant proportion of 6.4%, $P < 0.05$). The former trend was more
242 evident in the northern and western (high altitude permafrost areas) of the Tibetan Plateau,
243 while the latter was concentrated in the central regions (Figure 1a,c).

244

245 3.2 Relationships between the EOS and climate variables

246 We first analyzed partial correlations between seasonal climate variables and the EOS
247 without using pre-seasons. In autumn, the EOS showed a significant positive correlation
248 with temperatures ($P < 0.05$) but a weak negative correlation with precipitation ($P > 0.05$)
249 across the Tibetan Plateau (Figure S1). The partial correlations between EOS and climatic
250 variables in other seasons were not statistically significant ($P > 0.05$).

251 We further analyzed the partial correlations between EOS and pre-season climatic
252 variables. Across the Tibetan Plateau, the regionally averaged EOS showed a weak
253 negative correlation with pre-season cumulative precipitation but a significant positive
254 correlation with pre-season maximum and minimum temperatures (Figure 2). Spatially,
255 the proportion of pixels displaying a negative correlation between EOS and pre-season
256 cumulative precipitation was approximately 52.1%, and that with a significant negative
257 relationship was approximately 7.6% (Figure 3a). The proportions of pixels showing a
258 positive relationship between EOS and pre-season maximum and minimum temperatures
259 were approximately 65.2% and 89.4%, respectively, and the proportions of pixels with a
260 significant ($P < 0.05$) positive relationship were 19.5% and 34.0%, respectively (Figure
261 3c,e).



262

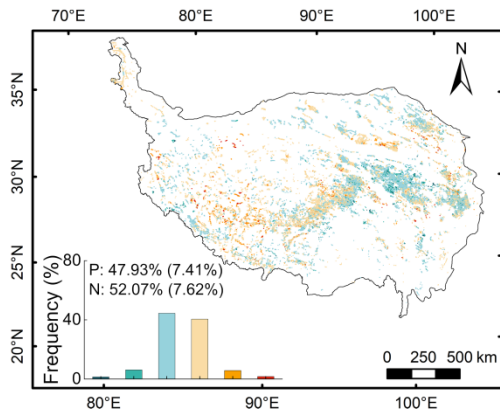
263

264

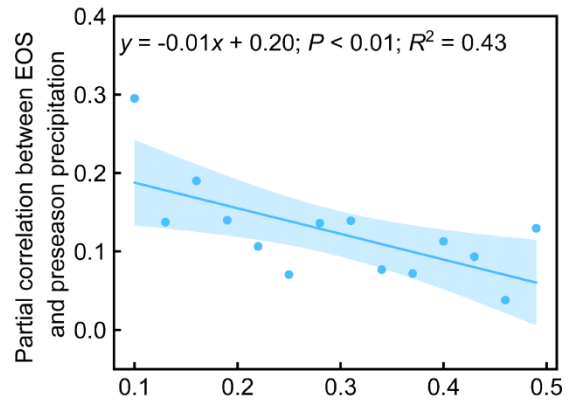
265

FIGURE 2 Partial correlation coefficients between pre-season climatic factors and EOS of marsh vegetation on the Tibetan Plateau. * $P < 0.05$; ** $P < 0.01$. Correlations lacking an asterisk are non-significant ($P > 0.05$).

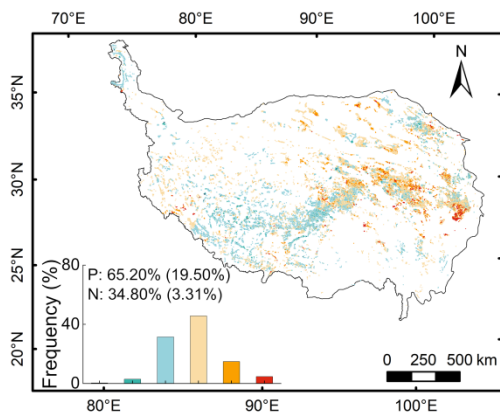
(a) EOS and preseason precipitation



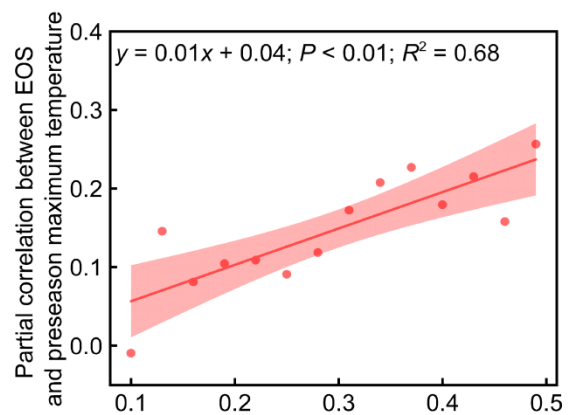
(b)



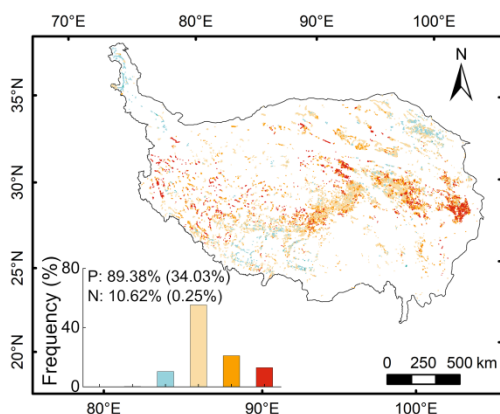
(c) EOS and preseason maximum temperature



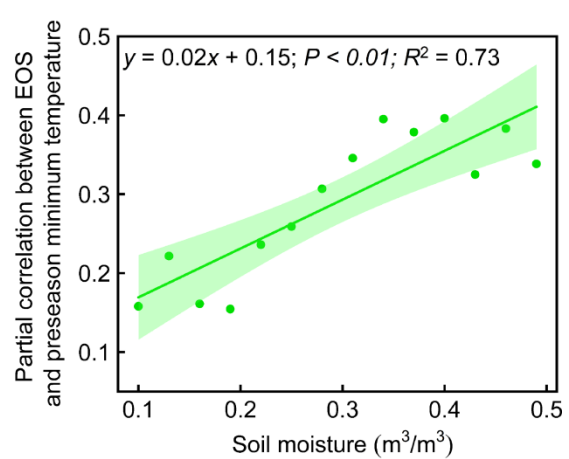
(d)



(e) EOS and preseason minimum temperature



(f)



266

267

268

269

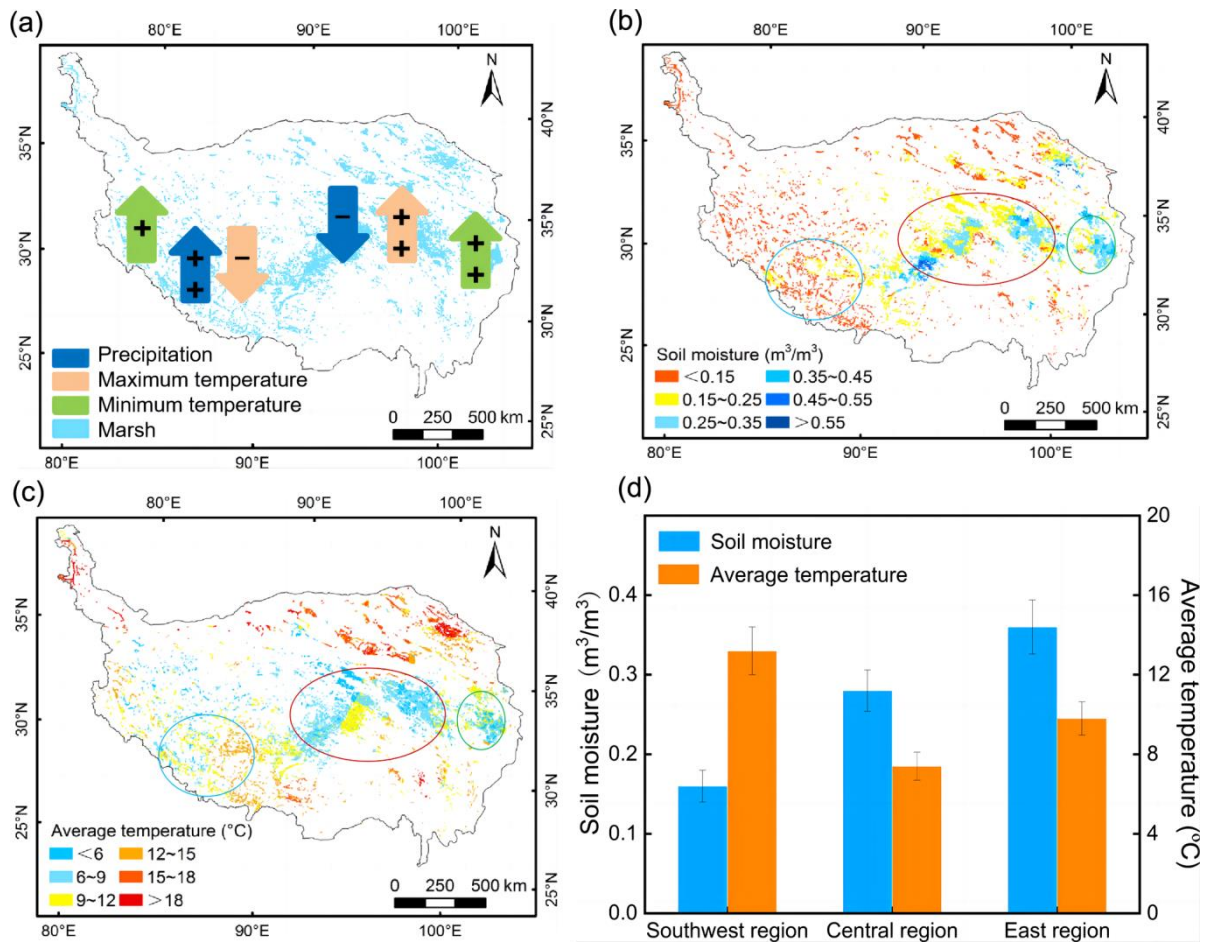
FIGURE 3 Relationship between EOS and preseason climate variables for the marshes on the Tibetan Plateau from 2001 to 2020. Spatial patterns of partial correlation coefficients between EOS and preseason cumulative precipitation (a), maximum

270 temperature (c), and minimum temperature (e). The changes in partial correlation
271 coefficients between EOS and pre-season cumulative precipitation (b), maximum
272 temperature (d), and minimum temperature (f) along the spatial gradient of long-term
273 pre-season soil moisture on the Tibetan Plateau from 2001 to 2020. The inset histograms
274 at the bottom of left figures (a, c, e) display the frequency distributions of partial
275 correlation coefficients. - and + show the negative and positive correlation, respectively;
276 * and ** indicate the correlation is significant ($P < 0.05$) and extremely significant ($P <$
277 0.01), respectively. The body lines in the right figures (b, d, f) indicate the linear fit for
278 the partial correlation coefficients, and the shading represents the 95% confidence band
279 of the fits.

280 The partial correlations between EOS and pre-season climatic variables indicated
281 spatial heterogeneity across the Tibetan Plateau. In the southwestern region, the EOS
282 showed a positive and negative partial correlation with pre-season cumulative
283 precipitation and pre-season maximum temperature, respectively; however, in the central
284 area, it exhibited a significant negative and positive partial correlation with these two
285 parameters, respectively (Figure 3a,c). The partial relationships between EOS and
286 pre-season minimum temperature were positive in most of the study area, and the positive
287 relationships were extremely significant ($P < 0.01$) in the western and eastern regions
288 (Figure 3e).

289 Subsequently, we examined the partial correlations between EOS and pre-season
290 climatic variables under different soil moisture levels in the study region (Figure 3). The

291 results showed that as the preseason soil moisture increased, the positive relationships
 292 between EOS and preseason cumulative precipitation gradually weakened, whereas those
 293 between EOS and preseason maximum and minimum temperatures became gradually
 294 stronger (Figures 3 and 4).



296 FIGURE 4 Impact of climate change on marsh EOS in different regions of the marshes
 297 on the Tibetan Plateau. (a) Conceptual diagrams showing the effects of climate change on
 298 the EOS. (b) Spatial distribution of long-term average preseason soil moisture (m^3/m^3).
 299 (c) The long-term average preseason temperature ($^{\circ}C$) for marsh vegetation on the Tibetan
 300 Plateau. (d) long-term average preseason soil moisture (m^3/m^3) and preseason
 301 temperature ($^{\circ}C$) in different regions of the Tibetan Plateau. “+” and “-” indicate that the

302 climatic variable had a significant positive and negative effect on the EOS, respectively
303 ($P < 0.05$). “++” indicates an extremely significant positive effect ($P < 0.01$). In the
304 southwestern Tibetan Plateau (circled in blue), increased pre-season precipitation can
305 significantly delay the EOS, while a higher pre-season maximum temperature will advance
306 it. In contrast, in the central Tibetan Plateau (circled in red), a higher pre-season maximum
307 temperature significantly delayed the EOS, while an increased pre-season precipitation
308 advanced it. In the eastern Tibetan Plateau (circled in green), a higher pre-season minimum
309 temperature significantly delayed the EOS.

310

311 **4 Discussions**

312 4.1 Autumn phenology of marsh vegetation on the Tibetan Plateau

313 The long-term average EOS for marsh vegetation occurred later in the eastern Tibetan
314 Plateau than in the central and southwestern regions (Figure 1b). This aligns with
315 observations that the eastern area has a lower altitude and a warmer climate (Shen et al.,
316 2021b), thus allowing the growing season to continue for longer. This result is consistent
317 with the findings of (Liu et al., 2021), which showed that the combined EOS for all
318 vegetation types occurred earlier in the central Tibetan Plateau and later in the eastern
319 regions. From 2001 to 2020, the average EOS was delayed by 4.10 days per decade across
320 the plateau (Figure 1c), a trend consistent with the results of Shen et al. (Shen et al., 2022),
321 which showed a delay of 8.2 days in the EOS for vegetation on the plateau over the same
322 period.

323 4.2 Climatic effects on the regionally averaged EOS for marsh vegetation

324 The regionally averaged EOS exhibited significant positive partial correlations with
325 pre-season daytime maximum and nighttime minimum temperatures but a weak negative
326 correlation with pre-season cumulative precipitation across the Tibetan Plateau. The
327 phenology of marsh vegetation on the plateau observed in this study differed from that of
328 grasslands reported in previous studies (Dorji et al., 2013; Shen et al., 2022; Yang et al.,
329 2021).

330 Previous studies have shown that in the grassland vegetation of the Tibetan Plateau,
331 increased precipitation significantly enhances water use efficiency, delaying the EOS. In
332 these relatively arid systems, the higher maximum temperatures increase evaporation and
333 reduce water use efficiency, thus advancing the EOS (Dorji et al., 2013; Yang et al., 2021).
334 In contrast, the marshes examined in the present study contained far more water
335 (Ganjurjav et al., 2022; Shen et al., 2022), making it less likely that pre-season
336 precipitation would affect the regionally averaged EOS for their vegetation, and explain
337 how the abundance of water allowed the EOS to be delayed by the increased pre-season
338 temperatures on the Tibetan Plateau.

339 Our results indicate that pre-season temperature is a key factor affecting the EOS, and
340 an increase in this parameter significantly delayed the EOS on the Tibetan Plateau (Figure
341 3). It is known that increased pre-season maximum temperature can promote
342 photosynthesis by enhancing the daytime photosynthetic activity of enzymes (Piao et al.,
343 2007; Turnbull et al., 2022). This increased photosynthesis, together with raised nighttime

344 minimum temperatures that reduce frost and low-temperature constraints (Shen et al.,
345 2016), would further delay the EOS on the plateau.

346

347 4.3 Elucidating spatial variations in the effects of climatic change on the EOS

348 We identified 3 characteristic areas within the Tibetan Plateau, which exhibited differing
349 primary drivers of the changes in EOS; south western, central and eastern.

350 In the relatively arid areas of the southwestern Tibetan Plateau, the EOS exhibited a
351 significant positive partial correlation with preseason cumulative precipitation but a
352 significant negative correlation with preseason maximum temperature (Figure 3a, c). This
353 indicated that, in this region, higher preseason precipitation significantly delayed the EOS
354 although this was constrained by preseason maximum temperatures tending to
355 significantly advance the EOS. As the climate in this southwestern region is dry and the
356 preseason soil moisture is low (Figure 4), an increase in preseason precipitation can
357 alleviate water stress, enhancing water use efficiency (Liu et al., 2016; Munné-Bosch et
358 al., 2004) and delaying the EOS. At the same time, an increase in maximum temperature
359 would increase hydrological losses through evaporation and reduce the amount of
360 available water (Kelsey et al., 2021; Shen et al., 2016), inhibiting the growth of marsh
361 vegetation. These dynamics fit well with our results, indicating that the EOS was
362 primarily affected by precipitation in the southwestern arid regions of the study area. For
363 the first time, our results indicate that, even in marsh ecosystems with their relatively high
364 water contents, available water may be insufficient for vegetation growth in the drier

365 regions of the Tibetan Plateau.

366 In the central Tibetan Plateau, a higher preseason temperature delayed the EOS,
367 while increased preseason precipitation advanced it (Figure 3). In the humid and cold
368 areas of the central Tibetan Plateau, soil moisture and temperature are higher and lower,
369 respectively, than those in the southwestern region (Cong et al., 2017) (Figure 4). In light
370 of these conditions, our results indicate that water was not the key factor affecting the
371 growth of marsh vegetation in the central Plateau, although temperature remained a
372 limiting factor.

373 An increase in maximum temperature can decelerate the process of chlorophyll
374 degradation (Shi et al., 2017) and retard the progression of leaf senescence (Estiarte et al.,
375 2017). In addition, high preseason nighttime temperatures reduce the occurrence of frost
376 damage (Shen et al., 2022). By calculating the number of the frost days, we confirmed
377 that warming preseason nighttime temperatures had the most notable negative effect on
378 the frost days in the central Tibetan Plateau, the coldest region of the study area (Figure
379 S2). This could account for the role of increasing minimum temperature in delaying the
380 EOS in the central Tibetan Plateau. In contrast, increased preseason precipitation could
381 retard the growth of marsh vegetation due to the accompanying cooling effect, which
382 would advance the EOS in the already cold and humid areas of the central Tibetan Plateau.

383 In the low altitude humid regions in the east and high-altitude cold permafrost regions
384 in the west, the EOS showed a significant positive correlation with preseason minimum
385 temperature (Figure 3), indicating that an increase in this parameter delayed the EOS in

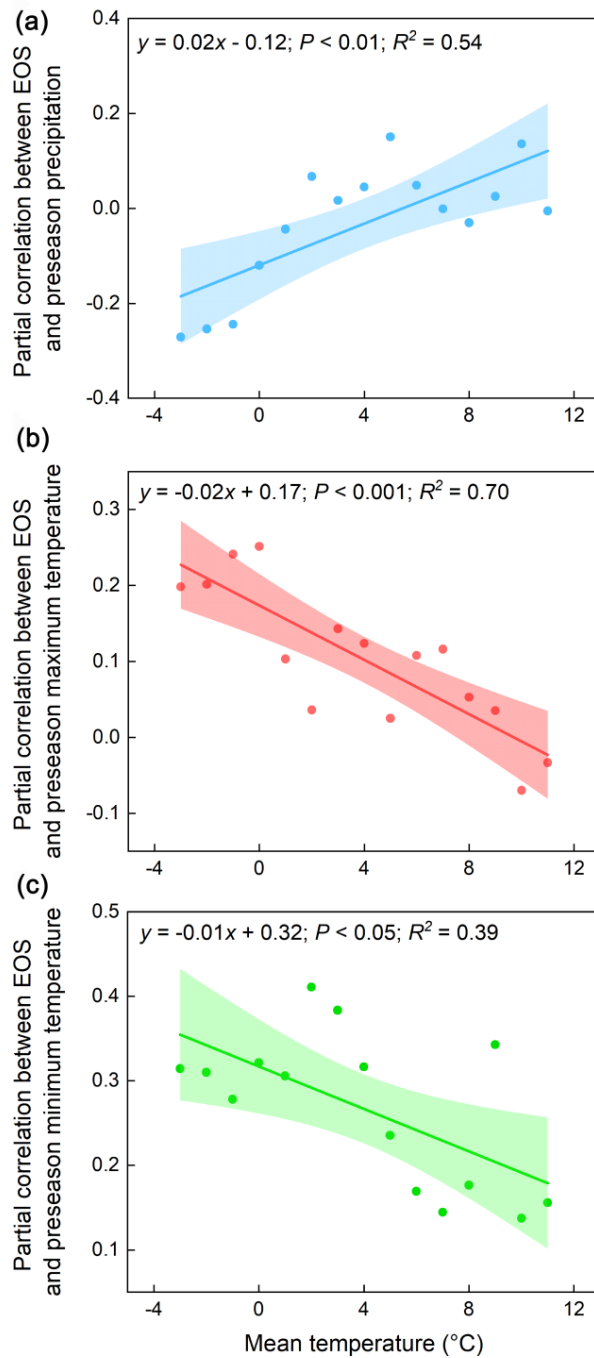
386 the marshes distributed in these regions of the Tibetan Plateau. However, the mechanisms
387 through which minimum temperature affects the EOS may differ between these two areas.
388 On one hand, increased nighttime temperatures cause a greater loss of organic matter due
389 to enhanced respiration, but on the other hand it can also stimulate accumulation of more
390 organic matter via the overcompensation effect (Shen et al., 2021b, 2022), a phenomenon
391 through which the vegetation recovers and exceeds its original state by promoting
392 photosynthesis the day after the enhanced respiration (Peng et al., 2013). It has been
393 reported that the occurrence of this effect is favored by the presence of sufficient water
394 and nutrients (Peng et al., 2013; Shen et al., 2022).

395 In cold high-altitude regions, the physiological processes causing vegetation
396 senescence are typically determined by low temperatures during cold nights (Tang et al.,
397 2016). In the high-altitude cold permafrost regions of the western Tibetan Plateau,
398 nighttime minimum temperature is generally low (Nan et al., 2005), and an increase in
399 pre-season minimum temperature would delay the EOS by alleviating frost damage and
400 retarding vegetation senescence (Cong et al., 2017). In contrast, in the low altitude areas
401 of the eastern Tibetan Plateau, the climate is relatively warm and humid (Figure 4) and
402 marsh vegetation has access to sufficient water (Shen et al., 2022). Therefore, although
403 organic matter may be depleted through the respiration of marsh vegetation due to
404 nighttime warming, increased temperatures can also promote photosynthesis, leading to
405 accumulation of more organic matter the following day via the over compensation effect
406 (Belsky et al., 1986; Shen et al., 2021b, 2022). This would contribute to delaying the EOS

407 in the eastern region as a consequence of the increased pre-season minimum temperatures.

408 By building a multi-variable regression for each pixel, we showed spatially which
409 pre-season variable is the most important for affecting the EOS. The results confirmed that
410 pre-season cumulative precipitation and minimum temperature played a crucial role in the
411 relatively arid southwestern and humid eastern Tibetan Plateau, respectively (Figure S3).
412 By comparing the partial correlation coefficients between EOS and climatic factors in
413 different regions, we confirmed that as annual mean temperature increased, the delaying
414 effects of higher pre-season maximum and minimum temperatures on the EOS gradually
415 weakened, while the delaying effect of increased pre-season precipitation became
416 gradually stronger (Figure 5). Based on our results, we propose that the effects of climate
417 variations on the EOS differ depending on the hydrological constraints on soil moisture
418 in the marshes within the Tibetan Plateau. As such, we further compared the partial
419 correlations between EOS and climatic factors for pre-season soil moisture gradients of
420 0.05 m³/m³. The results showed that as soil moisture increased, the delaying effect of
421 increased pre-season precipitation on the EOS gradually weakened (Figure 3), while the
422 delaying effects of higher pre-season maximum and minimum temperatures became
423 gradually stronger (Figure 3). This finding supports the proposal that increased
424 precipitation and warming temperatures significantly delayed the EOS for marsh
425 vegetation in the arid southwestern Tibetan Plateau and the humid central and eastern
426 areas, respectively. In contrast, increasing daytime temperatures and precipitation
427 advanced the EOS in the arid southwestern and humid central areas due to the reduced

428 soil moisture and cooling effect, respectively (Figure 3).



429

430 FIGURE 5 The changes in partial correlation coefficients between EOS and pre-season
431 cumulative precipitation, maximum temperature, and minimum temperature along the
432 spatial gradient of long-term annual mean temperature on the Tibetan Plateau from 2001
433 to 2020. The body lines in the figures indicate the linear fit for the partial correlation

434 coefficients, and the shading represents the 95% confidence band of the fits.

435

436 4.4 Attribution of temporal changes in the EOS

437 To further explain the temporal and spatial variations in the EOS, we calculated the rates

438 at which precipitation and maximum and minimum temperatures varied on the plateau

439 from 2001 to 2020 (Figure 6 and Table 1). The preseason cumulative precipitation and

440 maximum and minimum temperatures exhibited increasing trends (0.52 mm/a, 0.02 °C/a,

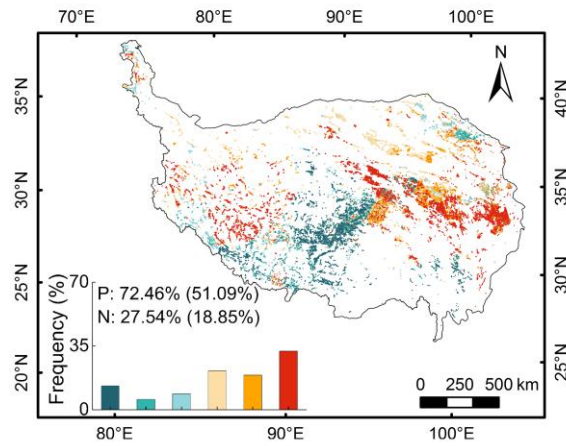
441 and 0.05 °C/a, respectively), but only the increase in the minimum temperature was

442 significant ($P < 0.05$). Because the EOS showed a significant positive relationship with

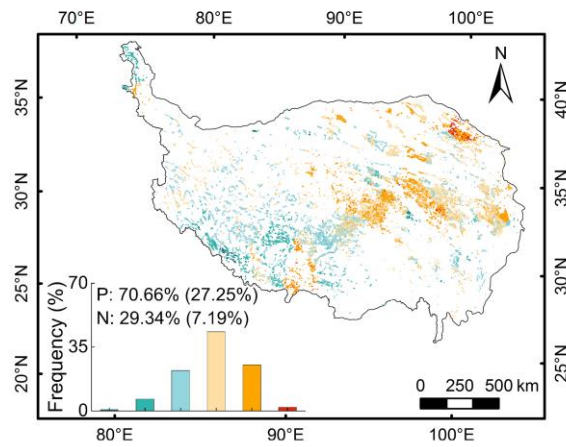
443 preseason minimum temperature, the increase in this parameter may partly account for

444 the delayed EOS on the Tibetan Plateau (Figure 1 and Table 1).

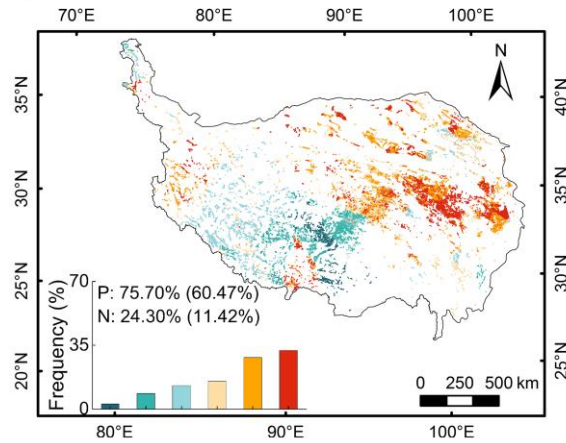
(a) Trend of pre-season precipitation (mm/a)



(b) Trend of pre-season maximum temperature ($^{\circ}\text{C}/\text{a}$)



(c) Trend of pre-season minimum temperature ($^{\circ}\text{C}/\text{a}$)



445

446 FIGURE 6 Pre-season climate change in the marshes of the Tibetan Plateau. Spatial

447 patterns of temporal trends in pre-season cumulative precipitation (a), maximum

448 temperature (b), and minimum temperature (c) in the marshes of the Tibetan Plateau from
 449 2001 to 2020. The inset histograms at the bottom of figures display the frequency
 450 distributions of the trends. - and + show the negative and positive trend, respectively; *
 451 and ** indicate the variation trend is significant ($P < 0.05$) and extremely significant (P
 452 < 0.01), respectively.

453 Table 1 Temporal trends of preseason and seasonal precipitation (mm/a), maximum
 454 temperature ($^{\circ}\text{C}/\text{a}$), and minimum temperature ($^{\circ}\text{C}/\text{a}$) in marshes of the Tibetan Plateau
 455 from 2001 to 2020.

	Precipitation	maximum temperature	minimum temperature
Preseason	0.52*	-0.02	0.05*
Spring	0.22	0.01	0.05**
Summer	0.31	0.05*	0.06*
Autumn	0.14	0.05	0.08**
Winter	0.79	-0.03	0.03

456 ** $P < 0.01$; * $P < 0.05$.

457 In the high-altitude arid area of the southwestern Tibetan Plateau, the EOS was
 458 positively correlated with preseason cumulative precipitation (Figure 3). As preseason
 459 cumulative precipitation showed significant increasing trends in the high-altitude arid
 460 area of the southwestern Tibetan Plateau (Figure 6), the increase in preseason
 461 precipitation may partly account for the delayed EOS in this region (Figure 1). In the low

462 altitude humid areas in the east and high-altitude cold permafrost areas in the west, the
463 EOS was positively correlated with preseason minimum temperature (Figure 3).
464 Therefore, we deduce that the extremely significant increases of preseason minimum
465 temperature may contribute to the delayed EOS in these regions (Figures 1 and 6). In the
466 northeastern area of the plateau, the EOS appeared to occur earlier throughout the study
467 period (Figure 1), possibly due to the rise in preseason minimum temperature (Figures 3
468 and 6).

469

470 **5 Conclusions**

471 Our study uncovers several crucial findings regarding the end of the growing season (EOS)
472 in marsh vegetation across the Tibetan Plateau. Firstly, we observed a significant delay in
473 the EOS by 4.10 days/decade during the study period. Secondly, while average preseason
474 cumulative precipitation did not notably impact the regionally averaged EOS, warmer
475 preseason temperatures led to a significant delay in the average EOS of marsh vegetation.
476 Notably, the delaying effect of higher nighttime temperatures on the regionally averaged
477 EOS was more pronounced than that of daytime temperatures. This asymmetric response
478 to diurnal temperature variations can be attributed to the widespread delaying effect of
479 nighttime warming and the spatially diverse relationship between EOS and daytime
480 temperature, influenced by water conditions. Furthermore, our evidence indicates that
481 hydrological factors influencing soil water content play a regulatory role in the impact of
482 climate change on the EOS. As soil moisture decreased, the delaying effect of increasing

483 preseason maximum temperatures gradually weakened and even reversed, while the
484 delaying effect of increased preseason precipitation was strengthened. In the humid, cold
485 regions of the central Tibetan Plateau, higher preseason maximum temperatures
486 significantly delayed the EOS, whereas increased precipitation advanced it, potentially
487 due to a cooling effect. In the low altitude, humid regions in the east, higher minimum
488 temperatures delayed the EOS, possibly due to an overcompensation effect. In the arid
489 southwestern area, increased precipitation directly and significantly delayed the EOS,
490 whereas higher daytime temperatures advanced it, likely due to limited water availability.
491 These findings suggest that the EOS in these regions is constrained by water conditions,
492 even within marsh ecosystems. Overall, our study highlights the asymmetric influences
493 of daytime and nighttime temperatures on the EOS of marsh vegetation, particularly in
494 the context of global diurnal asymmetric warming (stronger warming during nighttime
495 than during daytime). It underscores the importance of considering water conditions in
496 EOS simulations conducted by terrestrial ecosystem models in cold and dry regions
497 worldwide.

498

499 **Acknowledgements**

500 We gratefully acknowledge the National Natural Science Foundation of China
501 (42230516), Key Research Program of Frontier Sciences, Chinese Academy of Sciences
502 (ZDBS-LY-7019), and the Spanish Government grant TED2021-132627 B-I00, funded
503 by MCIN, AEI/10.13039/ 501100011033 European Union Next Generation EU/PRTR.

504

505 **Conflict of interest statement**

506 The authors declare no conflict of interest.

507

508 **Data availability statement**

509 The MOD13Q1 NDVI dataset was provided by the Earth Science Data Systems of the

510 National Aeronautics and Space Administration

511 (<https://ladsweb.modaps.eosdis.nasa.gov>). The distribution of marshes was obtained from

512 the wetland distribution datasets for China (<http://www.geodata.cn>). The climate data was

513 available from the National Meteorological Information Center of China

514 (<http://data.cma.cn/data>). The soil moisture data were obtained from the National Tibetan

515 Plateau Scientific Data Center (<https://data.tpdc.ac.cn>).

516

517 **References**

518 Bao, G., Tuya, A., Bayarsaikhan, S., Dorjsuren, A., Mandakh, U., Bao, Y., Li, C., &

519 Vanchindorj, B. (2020). Variations and climate constraints of terrestrial net primary

520 productivity over Mongolia. *Quaternary International*, 537, 112-125.

521 <https://doi.org/10.1016/j.quaint.2019.06.017>

522 Belsky, A. J. (1986). Does herbivory benefit plants? A review of the evidence. *The*

523 *American Naturalist*, 127, 870-892. <https://doi.org/10.1086/284531>

524 Che, M., Chen, B., Innes, J. L., Wang, G., Dou, X., Zhou, T., Zhang, H., Yan, J., Xu, G.,

525 & Zhao, H. (2014). Spatial and temporal variations in the end date of the vegetation

526 growing season throughout the Qinghai–Tibetan Plateau from 1982 to 2011.
527 *Agricultural and Forest Meteorology*, 189, 81-90.
528 <https://doi.org/10.1016/j.agrformet.2014.01.004>

529 Chen, X. (2017). Plant phenology of natural landscape dynamics. In Spatiotemporal
530 processes of plant phenology. Springer, Berlin, Heidelberg.

531 Chen, X., An, S., Inouye, D. W., & Schwartz, M. D. (2015). Temperature and snowfall
532 trigger alpine vegetation green-up on the world's roof. *Global Change Biology*, 21,
533 3635-3646. <https://doi.org/10.1111/gcb.12954>

534 Cheng, M., Jin, J., & Jiang, H. (2021). Strong impacts of autumn phenology on grassland
535 ecosystem water use efficiency on the Tibetan Plateau. *Ecological Indicators*, 126,
536 107682. <https://doi.org/10.1016/j.ecolind.2021.107682>

537 Coleman, D. J., Schuerch, M., Temmerman, S., Guntenspergen, G., Smith, C. G., &
538 Kirwan, M. L. (2022). Reconciling models and measurements of marsh vulnerability
539 to sea level rise. *Limnology and Oceanography Letters*, 7, 140-149.
540 <https://doi.org/10.1002/lol2.10230>

541 Cong, N., Shen, M., & Piao, S. (2017). Spatial variations in responses of vegetation
542 autumn phenology to climate change on the Tibetan Plateau. *Journal of Plant*
543 *Ecology*, 10, 744-752. <https://doi.org/10.1093/jpe/rtw084>

544 Cong, N., Wang, T., Nan, H., Ma, Y., Wang, X., Myneni, R. B., & Piao, S. (2013). Changes
545 in satellite-derived spring vegetation green-up date and its linkage to climate in
546 China from 1982 to 2010: a multimethod analysis. *Global Change Biology*, 19, 881-

547 891. <https://doi.org/10.1111/gcb.12077>

548 Dong, M., Jiang, Y., Zheng, C., & Zhang, D. (2012). Trends in the thermal growing season
549 throughout the Tibetan Plateau during 1960-2009. *Agricultural and Forest*
550 *Meteorology*, *166*, 201-206. <https://doi.org/10.1016/j.agrformet.2012.07.013>

551 Dorji, T., Totland, Ø., Moe, S. R., Hopping, K. A., Pan, J., & Klein, J. A. (2013). Plant
552 functional traits mediate reproductive phenology and success in response to
553 experimental warming and snow addition in Tibet. *Global Change Biology*, *19*, 459-
554 472. <https://doi.org/10.1111/gcb.12059>

555 Estiarte, M., & Peñuelas, J. (2015). Alteration of the phenology of leaf senescence and
556 fall in winter deciduous species by climate change: effects on nutrient proficiency.
557 *Global change biology*, *21*, 1005-1017. <https://doi.org/10.1111/gcb.12804>

558 Fu, Y. H., Piao, S., Delpierre, N., Hao, F., Hänninen, H., Liu, Y., Sun, W., Janssens, I. A.,
559 & Campioli, M. (2018). Larger temperature response of autumn leaf senescence than
560 spring leaf - out phenology. *Global Change Biology*, *24*(5), 2159-2168.
561 <https://doi.org/10.1111/gcb.14021>

562 Fu, Y. H., Piao, S., Op de Beeck, M., Cong, N., Zhao, H., Zhang, Y., Menzel, A., &
563 Janssens, I. A. (2014). Recent spring phenology shifts in western Central Europe
564 based on multiscale observations. *Global Ecology and Biogeography*, *23*, 1255-1263.
565 <https://doi.org/10.1111/geb.12210>

566 Ganguly, S., Friedl, M. A., Tan, B., Zhang, X., & Verma, M. (2010). Land surface
567 phenology from MODIS: Characterization of the Collection 5 global land cover

568 dynamics product. *Remote Sensing of Environment*, 114, 1805-1816.
569 <https://doi.org/10.1016/j.rse.2010.04.005>

570 Ganjurjav, H., Gornish, E. S., Hu, G., Schwartz, M. W., Wan, Y., Li, Y., & Gao, Q. (2020).
571 Warming and precipitation addition interact to affect plant spring phenology in
572 alpine meadows on the central Qinghai-Tibetan Plateau. *Agricultural and Forest
573 Meteorology*, 287, 107943. <https://doi.org/10.1016/j.agrformet.2020.107943>

574 Gao, Y. C., & Liu, M. (2013). Evaluation of high-resolution satellite precipitation
575 products using rain gauge observations over the Tibetan Plateau. *Hydrology and
576 Earth System Sciences*, 17, 837-849. <https://doi.org/10.5194/hess-17-837-2013>

577 Garonna, I., De Jong, R., De Wit, A. J., Mùcher, C. A., Schmid, B., & Schaepman, M. E.
578 (2014). Strong contribution of autumn phenology to changes in satellite - derived
579 growing season length estimates across Europe (1982-2011). *Global Change
580 Biology*, 20, 3457-3470. <https://doi.org/10.1111/gcb.12625>

581 Ge, Q., Wang, H., Rutishauser, T., & Dai, J. (2015). Phenological response to climate
582 change in China: a meta - analysis. *Global change biology*, 21(1), 265-274.
583 <https://doi.org/10.1111/gcb.12648>

584 Kelsey, K. C., Pedersen, S. H., Leffler, A. J., Sexton, J. O., Feng, M., & Welker, J. M.
585 (2021). Winter snow and spring temperature have differential effects on vegetation
586 phenology and productivity across Arctic plant communities. *Global Change
587 Biology*, 27, 1572-1586. <https://doi.org/10.1111/gcb.15505>

588 Keppeler, F. W., Olin, J. A., López - Duarte, P. C., Polito, M. J., Hooper - Bùì, L. M.,

589 Taylor, S. S., Rabalais, N. N., Fodrie F. J., Roberts, B. J., Turner, R. R., Matin, C.
590 W., & Jensen, O. P. (2021). Body size, trophic position, and the coupling of different
591 energy pathways across a saltmarsh landscape. *Limnology and Oceanography*
592 *Letters*, 6, 360-368. <https://doi.org/10.1002/lol2.10212>

593 Li, Q., Shi, G., Shanguan, W., Nourani, V., Li, J., Li, L., Huang, F., Zhang, Y., Wang, C.,
594 Wang, D., Qiu, J., Lu, X., & Dai, Y. (2022). A 1 km daily soil moisture dataset over
595 China using in situ measurement and machine learning, *Earth Syst. Sci. Data*, 14,
596 5267–5286. <https://doi.org/10.5194/essd-14-5267-2022>

597 Liu, Q., Fu, Y. H., Zeng, Z., Huang, M., Li, X., & Piao, S. (2016). Temperature,
598 precipitation, and insolation effects on autumn vegetation phenology in temperate
599 China. *Global Change Biology*, 22, 644-655. <https://doi.org/10.1111/gcb.13081>

600 Liu, X., Chen, Y., Li, Z., Li, Y., Zhang, Q., & Zan, M. (2021). Driving Forces of the
601 Changes in Vegetation Phenology in the Qinghai–Tibet Plateau. *Remote Sensing*, 13,
602 4952. <https://doi.org/10.3390/rs13234952>

603 Ma, R., Shen, X., Zhang, J., Xia, C., Liu, Y., Wu, L., Wang, Y., Jiang, M., & Lu, X. (2022).
604 Variation of vegetation autumn phenology and its climatic drivers in temperate
605 grasslands of China. *International Journal of Applied Earth Observation and*
606 *Geoinformation*, 114, 103064. <https://doi.org/10.1016/j.jag.2022.103064>

607 Mao, D., Wang, Z., Du, B., Li, L., Tian, Y., Jia, M., Zeng, Y., Song, K., Jiang, M., & Wang,
608 Y. (2020). National wetland mapping in China: A new product resulting from object-
609 based and hierarchical classification of Landsat 8 OLI images. *ISPRS Journal of*

610 *Photogrammetry and Remote Sensing*, 164, 11-25.
611 <https://doi.org/10.1016/j.isprsjprs.2020.03.020>

612 Molino, G. D., Carr, J. A., Ganju, N. K., & Kirwan, M. L. (2022). Variability in marsh
613 migration potential determined by topographic rather than anthropogenic constraints
614 in the Chesapeake Bay region. *Limnology and Oceanography Letters*, 7, 321-331.
615 <https://doi.org/10.1002/lol2.10262>

616 Munné-Bosch, S., & Alegre, L. (2004). Die and let live: leaf senescence contributes to
617 plant survival under drought stress. *Functional Plant Biology*, 31, 203-216.
618 <https://doi.org/10.1071/FP03236>

619 Nan, Z., Li, S., & Cheng, G. (2005). Prediction of permafrost distribution on the Qinghai-
620 Tibet Plateau in the next 50 and 100 years. *Science in China Series D: Earth Sciences*,
621 48, 797-804. <https://doi.org/10.1360/03yd0258>

622 Peng, S., Piao, S., Ciais, P., Myneni, R. B., Chen, A., Chevallier, F., Dolman, A. J.,
623 Janssens, I. A., Penuelas, J., Zhang, G., Vicca, S., Wan, S., Wang, S., & Zeng, H.
624 (2013). Asymmetric effects of daytime and night-time warming on Northern
625 Hemisphere vegetation. *Nature*, 501, 88-92. <https://doi.org/10.1038/nature12434>

626 Peñuelas, J., Filella, I. (2001). Responses to a warming world. *Science*, 294(5543): 793-
627 795. <https://doi.org/10.1126/science.10668>.

628 Piao, S., Ciais, P., Friedlingstein, P., Peylin, P., Reichstein, M., Luysaert, S., Margolis,
629 H., Fang, J., Barr, A., Chen, A., Grelle, A., Hollinger, D. Y., Laurila, T., Lindroth, A.,
630 Richardson, A. D., & Vesala, T. (2008). Net carbon dioxide losses of northern

631 ecosystems in response to autumn warming. *Nature*, 451, 49-52.
632 <https://doi.org/10.1038/nature06444>

633 Piao, S., Cui, M., Chen, A., Wang, X., Ciais, P., Liu, J., & Tang, Y. (2011). Altitude and
634 temperature dependence of change in the spring vegetation green-up date from 1982
635 to 2006 in the Qinghai-Xizang Plateau. *Agricultural and Forest Meteorology*, 151,
636 1599-1608. <https://doi.org/10.1016/j.agrformet.2011.06.016>

637 Piao, S., Fang, J., & He, J. (2006a). Variations in vegetation net primary production in the
638 Qinghai-Xizang Plateau, China, from 1982 to 1999. *Climatic Change*, 74, 253-267.
639 <https://doi.org/10.1007/s10584-005-6339-8>

640 Piao, S., Fang, J., Zhou, L., Ciais, P., & Zhu, B. (2006b). Variations in satellite-derived
641 phenology in China's temperate vegetation. *Global Change Biology*, 12, 672-685.
642 <https://doi.org/10.1111/j.1365-2486.2006.01123.x>

643 Piao, S., Friedlingstein, P., Ciais, P., Viovy, N., & Demarty, J. (2007). Growing season
644 extension and its impact on terrestrial carbon cycle in the Northern Hemisphere over
645 the past 2 decades. *Global Biogeochemical Cycles*, 21.
646 <https://doi.org/10.1029/2006GB002888>

647 Piao, S., Liu, Q., Chen, A., Janssens, I. A., Fu, Y., Dai, J., Liu, L., Lian, X., Shen, M., &
648 Zhu, X. (2019). Plant phenology and global climate change: Current progresses and
649 challenges. *Global Change Biology*, 25, 1922-1940.
650 <https://doi.org/10.1111/gcb.14619>

651 Qin, G., Adu, B., Li, C., & Wu, J. (2022). Diverse Responses of Phenology in Multi-

652 Grassland to Environmental Factors on Qinghai–Tibetan Plateau in China.
653 *Theoretical and Applied Climatology*, 148, 931-942.
654 <https://doi.org/10.1007/s00704-022-03963-3>

655 Rice, K. E., Montgomery, R. A., Stefanski, A., Rich, R. L., & Reich, P. B. (2018).
656 Experimental warming advances phenology of groundlayer plants at the boreal -
657 temperate forest ecotone. *American journal of botany*, 105, 851-861.
658 <https://doi.org/10.1002/ajb2.1091>

659 Richardson, A. D., Keenan, T. F., Migliavacca, M., Ryu, Y., Sonnentag, O., & Toomey,
660 M. (2013). Climate change, phenology, and phenological control of vegetation
661 feedbacks to the climate system. *Agricultural and Forest Meteorology*, 169, 156-173.
662 <https://doi.org/10.1016/j.agrformet.2012.09.012>

663 Shen, M., Piao, S., Chen, X., An, S., Fu, Y. H., Wang, S., Cong, N., & Janssens, I. A.
664 (2016). Strong impacts of daily minimum temperature on the green-up date and
665 summer greenness of the Tibetan Plateau. *Global Change Biology*, 22, 3057-3066.
666 <https://doi.org/10.1111/gcb.13301>

667 Shen, M., Piao, S., Cong, N., Zhang, G., & Janssens, I. A. (2015a). Precipitation impacts
668 on vegetation spring phenology on the Tibetan Plateau. *Global Change Biology*, 21,
669 3647-3656. <https://doi.org/10.1111/gcb.12961>

670 Shen, M., Piao, S., Dorji, T., Liu, Q., Cong, N., Chen, X., An, S., Wang, S., Wang, T., &
671 Zhang, G. (2015b). Plant phenological responses to climate change on the Tibetan
672 Plateau: research status and challenges. *National Science Review*, 2, 454-467.

673 <https://doi.org/10.1093/nsr/nwv058>

674 Shen, M., Tang, Y., Chen, J., Zhu, X., & Zheng, Y. (2011). Influences of temperature and
675 precipitation before the growing season on spring phenology in grasslands of the
676 central and eastern Qinghai-Tibetan Plateau. *Agricultural and Forest Meteorology*,
677 *151*, 1711-1722. <https://doi.org/10.1016/j.agrformet.2011.07.003>

678 Shen, M., Wang, S., Jiang, N., Sun, J., Cao, R., Ling, X., Fang, B., Zhang, L., Zhang, L.,
679 Xu, X., Lv, W., Li, B., Sun, Q., Meng, F., Jiang, Y., Dorji, T., Fu, Y., Iier, A., Vitasse,
680 Y., Steltzer, H., Ji, Z., Zhao, W., Piao, S., & Fu, B. (2022). Plant phenology changes
681 and drivers on the Qinghai–Tibetan Plateau. *Nature Reviews Earth & Environment*,
682 *1-19*. <https://doi.org/10.1038/s43017-022-00317-5>

683 Shen, M., Zhang, G., Cong, N., Wang, S., Kong, W., & Piao, S. (2014). Increasing
684 altitudinal gradient of spring vegetation phenology during the last decade on the
685 Qinghai–Tibetan Plateau. *Agricultural and Forest Meteorology*, *189*, 71-80.
686 <https://doi.org/10.1016/j.agrformet.2014.01.003>

687 Shen, X., Jiang, M., & Lu, X. (2023). Diverse impacts of day and night temperature on
688 spring phenology in freshwater marshes of the Tibetan Plateau. *Limnology and*
689 *Oceanography Letters*, 1-7. <https://doi.org/10.1002/lol2.10285>

690 Shen, X., Jiang, M., Lu, X., Liu, X., Liu, B., Zhang, J., Wang, X., Tong, S., Lei, G., Wang,
691 S., Tong, C., Fan, H., Tian, K., Wang, X., Hu, Y., Xie, Y., Ma, M., Zhang, S., Cao,
692 C., & Wang, Z. (2021a). Aboveground biomass and its spatial distribution pattern of
693 herbaceous marsh vegetation in China. *Science China Earth Sciences*, *64*, 1115-1125.

694 <https://doi.org/10.1007/s11430-020-9778-7>

695 Shen, X., Liu, B., Henderson, M., Wang, L., Wu, Z., Wu, H., Jiang, M., & Lu, X. (2018).
696 Asymmetric effects of daytime and nighttime warming on spring phenology in the
697 temperate grasslands of China. *Agricultural and Forest Meteorology*, 259, 240-249.
698 <https://doi.org/10.1016/j.agrformet.2018.05.006>

699 Shen, X., Liu, B., Jiang, M., Wang, Y., Wang, L., Zhang, J., & Lu, X. (2021b).
700 Spatiotemporal change of marsh vegetation and its response to climate change in
701 China from 2000 to 2019. *Journal of Geophysical Research: Biogeosciences*, 126,
702 e2020JG006154. <https://doi.org/10.1029/2020JG006154>

703 Shen, X., Liu, B., Xue, Z., Jiang, M., Lu, X., & Zhang, Q. (2019). Spatiotemporal
704 variation in vegetation spring phenology and its response to climate change in
705 freshwater marshes of Northeast China. *Science of the Total Environment*, 666, 1169-
706 1177. <https://doi.org/10.1016/j.scitotenv.2019.02.265>

707 Shen, X., Liu, Y., Zhang, J., Wang, Y., Ma, R., Liu, B., Lu, X., & Jiang, M. (2022).
708 Asymmetric impacts of diurnal warming on vegetation carbon sequestration of
709 marshes in the Qinghai Tibet Plateau. *Global Biogeochemical Cycles*, 36,
710 e2022GB007396. <https://doi.org/10.1029/2022GB007396>

711 Shi, C., Sun, G., Zhang, H., Xiao, B., Ze, B., Zhang, N., & Wu, N. (2014). Effects of
712 warming on chlorophyll degradation and carbohydrate accumulation of alpine
713 herbaceous species during plant senescence on the Tibetan Plateau. *PLoS One*, 9,
714 e107874. <https://doi.org/10.1371/journal.pone.0107874>

-
- 715 Su, M., Huang, X., Xu, Z., Zhu, W., & Lin, Z. (2022). A Decrease in the Daily Maximum
716 Temperature during Global Warming Hiatus Causes a Delay in Spring Phenology in
717 the China–DPRK–Russia Cross-Border Area. *Remote Sensing*, *14*, 1462.
718 <https://doi.org/10.3390/rs14061462>
- 719 Tang, J., Körner, C., Muraoka, H., Piao, S., Shen, M., Thackeray, S. J., & Yang, X. (2016).
720 Emerging opportunities and challenges in phenology: a review. *Ecosphere*, *7*,
721 e01436. <https://doi.org/10.1002/ecs2.1436>
- 722 Turnbull, M. H., Murthy, R., & Griffin, K. L. (2002). The relative impacts of daytime and
723 night - time warming on photosynthetic capacity in *Populus deltoides*. *Plant, Cell*
724 *& Environment*, *25*, 1729-1737. <https://doi.org/10.1046/j.1365-3040.2002.00947.x>
- 725 Wang, Y., Shen, X., Jiang, M., Tong, S., & Lu, X. (2021). Spatiotemporal change of
726 aboveground biomass and its response to climate change in marshes of the Tibetan
727 Plateau. *International Journal of Applied Earth Observation and Geoinformation*,
728 *102*, 102385. <https://doi.org/10.1016/j.jag.2021.102385>
- 729 Wu, C., Peng, J., Ciais, P., Peñuelas, J., Wang, H., Beguería, S., Andrew Black, T., Jassal,
730 R. S. , Zhang, X. , Yuan, W., Liang, E. , Wang, X., Hua, H., Liu, R. , Ju, W., Fu, Y.,
731 & Ge, Q. (2022). Increased drought effects on the phenology of autumn leaf
732 senescence. *Nature Climate Change*, *12(10)*, 943-949.
733 <https://doi.org/10.1038/s41558-022-01464-9>
- 734 Wu, C., Wang, X., Wang, H., Ciais, P., Peñuelas, J., Myneni, R. B., Desai, A. R., Gough,
735 C. M., Gonsamo, A., Black, A. T., Jassal, R. S., Ju, W., Yuan, W., Fu, Y., Shen, M.,

736 li, S., Liu, R., Chen, J., & Ge, Q. (2018). Contrasting responses of autumn-leaf
737 senescence to daytime and night-time warming. *Nature Climate Change*, 8, 1092-
738 1096. <https://doi.org/10.1038/s41558-018-0346-z>

739 Yang, Y., Guan, H., Shen, M., Liang, W., & Jiang, L. (2015). Changes in autumn
740 vegetation dormancy onset date and the climate controls across temperate
741 ecosystems in China from 1982 to 2010. *Global Change Biology*, 21, 652-665.
742 <https://doi.org/10.1111/gcb.12778>

743 Yang, Y., Qi, N., Zhao, J., Meng, N., Lu, Z., Wang, X., Kang, L., Li, R., Ma, J., & Zheng,
744 H. (2021). Detecting the Turning Points of Grassland Autumn Phenology on the
745 Qinghai-Tibetan Plateau: Spatial Heterogeneity and Controls. *Remote Sensing*, 13,
746 4797. <https://doi.org/10.3390/rs13234797>

747 Yu, H., Luedeling, E., & Xu, J. (2010). Winter and spring warming result in delayed
748 spring phenology on the Tibetan Plateau. *Proceedings of the National Academy of*
749 *Sciences*, 107(51), 22151-22156. <https://doi.org/10.1073/pnas.1012490107>

750 Zhang, G., Zhang, Y., Dong, J., & Xiao, X. (2013). Green-up dates in the Tibetan Plateau
751 have continuously advanced from 1982 to 2011. *Proceedings of the National*
752 *Academy of Sciences*, 110, 4309-4314. <https://doi.org/10.1073/pnas.1210423110>

753 Zhu, W., Tian, H., Xu, X., Pan, Y., Chen, G., & Lin, W. (2012). Extension of the growing
754 season due to delayed autumn over mid and high latitudes in North America during
755 1982–2006. *Global Ecology and Biogeography*, 21, 260-271.
756 <https://doi.org/10.1111/j.1466-8238.2011.00675.x>